Excitation of $O(^3S)$ resonance radiation in inelastic collisions between $O(^5S)$ metastables and O_2 and N_2 gases

H. U. Kiefl, W. L. Borst,* and J. Fricke
Physikalisches Institut der Universität Würzburg Am Hubland, 8700 Würzburg, Federal Republic of Germany
(Received 24 July 1979)

The excitation of the ^3S state of atomic oxygen with subsequent emission of 1304-Å resonance radiation was observed in inelastic collisions between $O(^5S)$ metastables and O_2 and N_2 molecules according to the process $O(^5S)+X\rightarrow O(^3S)+X\rightarrow O(^3P)+X+h\nu(1304\text{ Å})$, where X is O_2 or N_2. The cross section for this endothermic process was measured for metastable kinetic energies from threshold at 0.5 eV to about 10 eV (laboratory frame). For O_2 as the target molecule, the cross section rose steeply from threshold to a plateau value of about $(3\pm1.5)\times10^{-17}$ cm^2 near 3 eV, from where it decreased slightly towards the maximum metastable kinetic energies available in the present experiment. For N_2 as the target, the corresponding cross section was at least a factor of 30 smaller. The $O(^5S)$ metastables were produced by electron impact dissociation of O_2 in a pulsed source and subsequently velocity selected with a time-of-flight method. The metastable beam was monitored by spontaneous decay of metastables in the target cell resulting in 1356-Å radiation. The excited $O(^3S)$ atoms produced in collisions with the target gas were monitored via 1304-Å resonance radiation.

I. INTRODUCTION

Collisions between metastable $O(^5S)$ atoms and O_2 and N_2 targets leading to sensitized fluorescence of 1304-Å radiation from $O(^3S)$ have been studied in the present work. The experiment made use of a velocity-selected metastable beam and a new vacuum-uv filter technique. The collision process leading to sensitized fluorescence of 1304-Å resonance radiation is very efficient with O_2 as the gas target. Cross sections on the order of several times 10^{-17} cm^2 at a few eV metastable kinetic energy have been observed in this case. When N_2 is used as the target gas, the corresponding cross section for exciting $O(^3S)$ state is smaller by at least a factor of 30.

In the past, the $O(^1S)$ metastable state has been studied by observing light from collisional quenching in gas discharges at relatively high pressures,[1-5] but not in atomic beam experiments as in the present work. There exist also quenching measurements in systems using metastable $O(^1D)$ atoms.[6,7] Only recently has work been initiated on the collisional deactivation of $O(^5S)$ metastables on various gas targets.[8,9] While these metastables are easily produced by electron impact dissociation[10,11] of O_2, the unique identification of them and their collision products in a beam experiment at low target-gas pressures poses some problems. These problems were overcome by the use of a new gas filter technique in the vacuum uv[12-17] that allowed the identification of $O(^5S)$ atoms by monitoring the 1356-Å radiation from their spontaneous decay and $O(^3S)$ atoms by 1304-Å resonance radiation (see Sec. II).

As a result of this gas filter technique, cross sections for sensitized fluorescence of $O(^3S)$ have been reported.[16] Furthermore, by improving the metastable source and the detection efficiency for vacuum-uv photons, the cross section for excitation of $O(^3S)$ in collisions with atmospheric and rare gases as well as for energy transfer into various rare-gas states was determined and reported elsewhere.[12,17-19]

The collision process of interest in the present work can be summarized as

$$O(^5S)+X+E_{kin}\rightarrow O(^3S)+X\rightarrow O(^3P)+h\nu(1304\text{ Å}), \quad (1)$$

where X is O_2 or N_2. The first step leading to $O(^3S)$ excitation is endothermic and the $O(^5S)$ excitation energy of 9.14 eV is used together with part of the center-of-mass energy in the $O(^5S)-X$ system to excitate the $O(^3S)$ resonance state. In the following, we describe the results concerning the processes given in Eq. (1). Additional results obtained with rare gases as the target gas X in Eq. (1) are reported elsewhere.[20]

It should be noted that the low-lying ^1D and ^1S states of atomic oxygen did not contribute to the production of 1304-Å photons in the present case because the required metastable kinetic energies necessary for the energy balance were not available. It is likely, however, that these metastable states were present in the beam, but they could not be detected because of their low excitation energies and long lifetimes.

II. EXPERIMENT AND MEASUREMENTS

A schematic diagram of the apparatus used in the present work is shown in Fig. 1. The $O(^5S)$ meta-

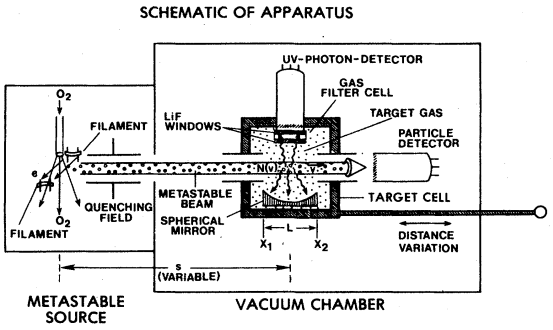

FIG. 1. Schematic of time-of-flight apparatus and uv photon detector. uv photons from spontaneous decay of metastables and collision products are monitored with a gas filter cell and single-photon counter. The photon signal is enhanced by means of a spherical mirror. Wavelength discrimination between 1356-Å radiation from spontaneous decay and 1304-Å radiation from O(^3S) is accomplished by using either N_2O or O_2 gas in the filter cell. Radiation from parts outside the region between x_1 and x_2 could not reach the detector.

stables were produced in the source by electron impact dissociation of O_2 at electron energies of about 100 eV. The metastable beam was defined to within 10^{-3} sr by apertures. A strong electric field of 15 kV/cm removed any charged particles from the beam and quenched long-lived atoms in high-lying Rydberg states.

After collimation the metastables entered the main vacuum chamber containing the target-gas cell. The metastables were detected by monitoring 1356-Å photons from the spontaneous decay of O(^5S) atoms in the target cell. (Metastables could also be detected with the axially mounted particle detector shown in Fig. 1, but for the present work only the vertically mounted uv- photon detector was used.) The photon detector also monitored the 1304-Å resonance radiation produced in the target cell as a result of collisions between O(^5S) metastables and the target gas.

The required wavelength discrimination between 1356- and 1304-Å photons was accomplished with a gas filter cell positioned between the interaction region of the beam and the photon detector. (The use of a vacuum-uv spectrometer was not possible owing to the extremely low intensity of only a few photons per second.) The filter gases used were N_2O and O_2. Figure 2 shows the transmission curves of these gases in the vacuum-uv region. It is seen that N_2O transmits the 1356-Å radiation with high efficiency, and O_2 as a filter gas transmits the 1304-Å resonance radiation. Nearly perfect discrimination exists between these two wavelengths owing to the dropoff in the transmission curves of the respective filter gases.

The end surfaces of the gas filter cell consisted of LiF windows, which had a transmission of 60% or greater for wavelengths longer than 1100 Å. Additional consistency checks concerning the wavelength discrimination were performed by using different window materials and changing the temperature of these materials in order to cover a range of wavelengths in the vacuum uv. Details of this procedure and the gas filter technique have also been described elsewhere.[8,13,16]

The optical viewing range in the target chamber that was "seen" by the photon detector was about 3 cm along the metastable beam. The efficiency for photon collection was increased by inserting a vacuum-uv mirror into the target-gas cell as shown in Fig. 1. This mirror was of spherical shape and was made of aluminum coated with magnesium fluoride.

The gas density in the target cell was determined with an ionization gauge connected to the main vac-

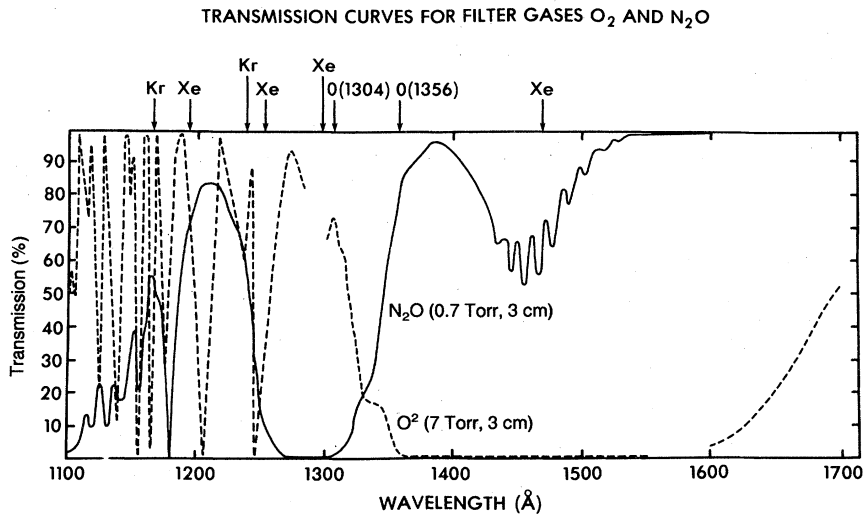

FIG. 2. Vacuum-uv transmission curves for N_2O and O_2 used in the filter cell of the uv photon detector. Effective discrimination exists between 1356- and 1304-Å photons.

uum chamber and by using the known pumping speeds and conductances of the entrance and exit tubes in the target cell. A separate indication for the target-gas density was obtained from a measurement of the target-gas consumption and the known pumping speeds and conductances. These two measurements agreed within the experimental error of 30%.

The time-of-flight (TOF) electronics and the data acquisition system that were used have been described elsewhere.[16] The on time of the electron gun in the metastable source was 24 μsec and the TOF channel width 8 μsec. The distance traveled by the metastables between source and target cell was about 31 cm.

A typical TOF spectrum of $O(^5S)$ metastables in the target chamber is shown in Fig. 3. This spectrum was obtained by monitoring the 1356-Å photons from the spontaneous decay of $O(^5S)$ metastables and will henceforth be called the "reference spectrum." It contained the velocity distribution from which the energy distribution of the metastable atoms and hence the collision energy were obtained. The reference spectrum was obtained with N_2O gas in the filter cell in front of the photon detector. Figure 3 shows also a "reaction spectrum" obtained by monitoring the 1304-Å radiation from $O(^3S)$ atoms that were excited in collisions between $O(^5S)$ and O_2 gas. In order to transmit the 1304-Å photons through the filter cell, O_2 was used as the filter gas (see also Fig. 2).

The rise in the reaction spectrum in Fig. 3 at channel 13 towards smaller channel numbers indicates that a minimum kinetic energy of the metastables was necessary to produce the 1304-Å radiation. This is consistent with the term level diagram of atomic oxygen shown in Fig. 4, which indicates that an energy of 0.36 eV is required for exciting the ^3S from the ^5S state. Thus the slow $O(^5S)$ metastables in the beam appearing in Fig. 3 at channel 14 and higher channels cannot contribute to the production of 1304-Å resonance radiation.

The working pressure in the target chamber was chosen as high as possible in order to obtain detectable signals. At the same time it was chosen sufficiently low for the experiment to remain in the single-collision domain. It was found that the 1304-Å signal was proportional to the gas pressure in the target chamber up to values of about 5×10^{-3} Torr. The photon signal reached a peak at about 1×10^{-2} Torr and decreased rapidly at higher pressures owing to beam attenuation near the entrance of the target chamber.

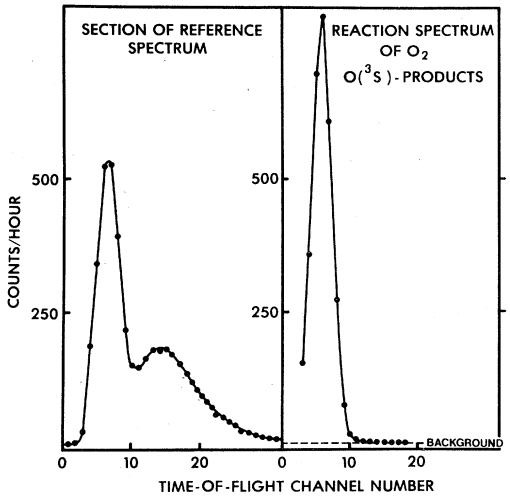

FIG. 3. Measured time-of-flight spectra. The time scale is 8 μsec/channel. The left spectrum represents the 1356-Å signal from spontaneous metastable decay in the target cell and thus contains the velocity distribution of metastables in the beam. The right spectrum is the 1304-Å signal from the $O(^3S)$ collision products. By dividing these spectra point by point, the cross section for $O(^3S)$ production was obtained as a function of metastable velocity or energy (see text).

III. DATA EVALUATION AND RESULTS

The counting rate for 1356-Å photons from spontaneous decay of $O(^5S)$ metastables in the presence

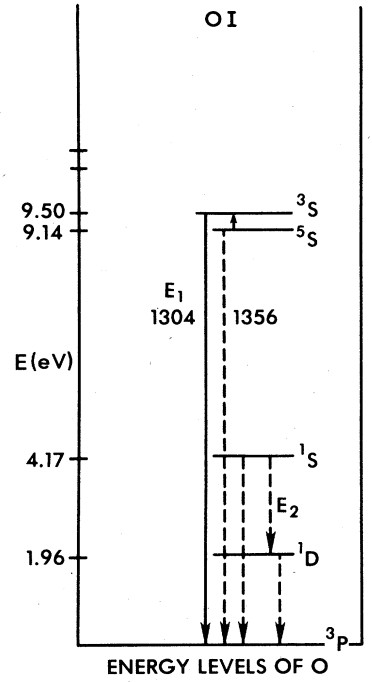

FIG. 4. Partial term level diagram of atomic oxygen showing the metastable states. The process studied is indicated by the short upward arrow. The uv radiation monitored from the ^3S and ^5S states is also indicated.

of target gas was given by (see also reference spectrum in Fig. 3)

$$R_{1356}(v)dv = CN_1(v)dv\frac{f}{v\tau}\int_{x_1}^{x_2}\exp\left[-\left(\frac{1}{v\tau}+N_T\sigma_t\right)x\right]dx\,, \tag{2}$$

where $N_1(v)$ is the number of metastables per beam pulse and velocity interval dv entering the target cell at x_1 (see Fig. 1), v the O(^{5}S) metastable velocity, τ the metastable lifetime ($\tau = 180$ μsec, see Ref. 14), f the repetition rate of the beam pulse, N_T the target-gas density, $\sigma_t(v)$ the total cross section for elastic and inelastic collisions in the target chamber, and C a constant containing the effective solid angle and efficiency of the photon-counting system.

The integral in Eq. (2) accounts for the loss of metastables due to spontaneous decay and elastic and inelastic scattering in the viewing region of the photon detector. The integration is carried out between the positions x_1 and x_2, as indicated in Fig. 1. The counting rate of 1304-Å photons (reaction spectrum in Fig. 3) was given by

$$R_{1304}(v)dv = CN_1(v)\sigma(v)dvfN_T \times\int_{x_1}^{x_2}\exp\left[-\left(\frac{1}{v\tau}+N_T\sigma_t\right)x\right]dx\,, \tag{3}$$

where $\sigma(v)$ is the inelastic cross section for the production of 1304-Å photons at the velocity v. The constant C occurring in Eqs. (2) and (3) is the same because the wavelengths 1356 and 1304 Å are sufficiently close together for the photon detection efficiencies to be the same. The velocity v in Eqs. (2) and (3) is the average velocity corresponding to the finite channel width. Possible uncertainties associated with the finite channel width are discussed in the appendix.

By dividing the two count rates in Eqs. (2) and (3) channel by channel, one obtains the desired cross section for 1304-Å photon production as a function of metastable velocity

$$\sigma(v) = (1/v\tau N_T)[R_{1304}(v)/R_{1356}(v)]. \tag{4}$$

All quantities on the right-hand side of this equation are known. The metastable velocity follows from the distance s between source and target chamber (see Fig. 1) and the time of flight. The velocities were converted to metastable kinetic energies in the laboratory frame. By plotting the resulting cross sections as a function of kinetic energy, the curves shown in Fig. 5 and Fig. 6 were obtained.

It is seen from Fig. 5 that the cross section for O(^3S) excitation from O(^{5}S) on O_2 rises steeply near the threshold of 0.5 eV (laboratory frame) and reaches the large value of 3×10^{-17} cm^2 at metastable kinetic energies of 3 eV. The cross section decreases slightly towards energies of 8 eV (which was the maximum energy available). The total uncertainty in the absolute cross section is about ±50% (see also the Appendix for a discussion of experimental errors).

The corresponding cross section for O(^{3}S) excitation from O(^{5}S) on N_2 is smaller by at least a factor of 30, as seen from Fig. 6. This difference seems plausible because the O(^{3}S) atoms appearing

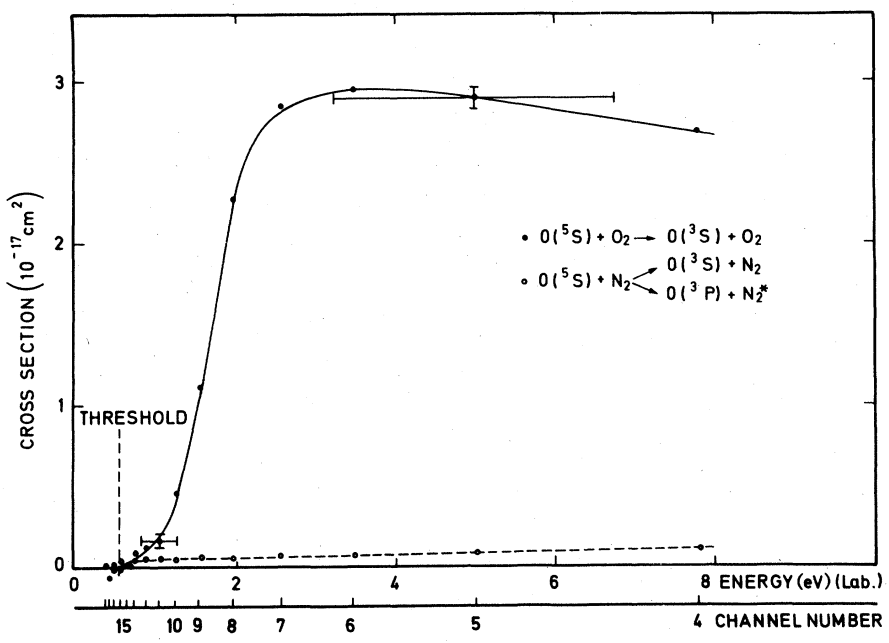

FIG. 5. Cross section for O(^{3}S) production by O(^{5}S) metastables on O_2 and N_2 as a function of metastable kinetic energy in the laboratory frame. The threshold for the endothermic process is indicated. The vertical error bars refer only to counting statistics. The horizontal error bars are comprised of the uncertainties in the metastable kinetic energy due to thermal motion of the target gas, finite pulse width, and finite size of the target chamber.

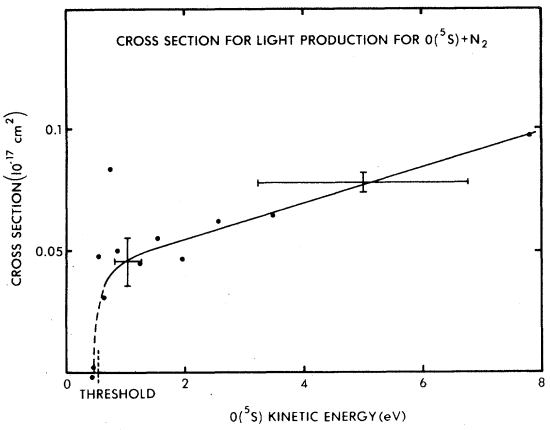

FIG. 6. Cross section for $O(^3S)$ excitation by $O(^5S)$ metastables on N_2 as a function of metastable kinetic energy with the scale expanded by a factor of 20 as comparted to Fig. 5. Threshold behavior is again observed.

in the exit channel of the reaction do not necessarily have to be identical with the entering $O(^5S)$ atoms. After forming an intermediate complex, each of the three participating O atoms could carry away the excitation energy in the $O(^3S)$ state. This is not possible with N_2 as the target gas, where the incoming and outgoing O atoms are the same. (It should be interesting in this regard to study the situation with NO as a target gas.)

The question arose whether the O_2 target-gas molecules were also excited in the collision according to the process

$$O(^5S)+O_2 \rightarrow O(^3S)+O_2^*, \quad (5)$$

with subsequent emission of detection of uv photons from O_2^*. This possibility was ruled out for the following reasons: First, the observed threshold of 0.5 eV in the cross section in Fig. 5 is very close to the minimum required energy of 0.36 eV in the center-of-mass system (see also Fig. 4). Second, test measurements were performed with N_2O in the uv gas filter cell either with or without O_2 in the target chamber. A CaF_2 window was used in these tests with a cutoff wavelength of about 1260 Å. Any photons in the range 1260–2400 Å could have been detected (except for a narrow absorption band in N_2O between 1260 and 1310 Å, see also Fig. 2) as the work function of the Cu-Be-O multiplier used was about 5 eV. In this way, only 1356-Å radiation from $O(^5S)$ could have been detected without the target gas present. It was found that the addition of O_2 as a target gas did not increase the photon count as would be expected with additional light from O_2^*. [Actually, a small decrease in the photon count was observed due to scattering losses of $O(^5S)$ atoms in the target chamber.] As mentioned before, no 1304-Å resonance radiation could reach the multiplier with N_2O as a filter gas. It was thus shown that no uv photons other than 1304-Å radiation were detected in the actual experiment with O_2 as a filter gas. (The detection of photons from the narrow 1260–1310-Å region was very unlikely.)

These tests are consistent with the fact that only strongly repulsive potential curves are reached in collisional excitation of O_2 up to excitation energies of about 10 eV. Thus a fast dissociation of O_2^* will take place without the emission of vacuum-uv photons. Any cascading transitions (which are unlikely) would disperse the available energy into a wavelength range not detectable in the present experiment. It was therefore concluded that the observed vacuum-uv signal with O_2 as a filter gas was due entirely to the emission of 1304-Å resonance radiation.

IV. CONCLUSIONS

The present work appears to be the first of its kind, in which an absolute cross section for excitation by a single species of metastables was measured as a function of metastable kinetic energy. In particular, the metastable species was uniquely identified and measurements were obtained from the threshold for the excitation process at a fraction of an eV up to nearly 8 eV. The previous measurements involving metastable beams were carried out at much higher energies, and the metastable species and beam composition were usually not uniquely identified. The present results show that excitation can take place with a large cross section at very low energies near the threshold for the endothermic process in question.

It is also important to note that the observed cross section for $O(^3S)$ excitation by $O(^5S)$ on O_2 is very large despite the fact that the process is not nearly resonant, as it involves an energy deficiency of 0.36 eV. This energy defect has to be provided by the kinetic energy of the $O(^5S)$ metastables. While most of the interaction energy is provided by the excitation energy of the ^5S state of atomic oxygen, the kinetic energy contribution is significant. This is for instance in marked distinction to most laser processes, where near-resonant excitation transfer occurs.

Note added in proof. An experimental procedure similar to that described here is being used at our institute to determine absolute cross sections for sensitized fluorescence of metastable atomic hydrogen in collisions with rare gases and molecules.[21]

ACKNOWLEDGMENTS

One of us (WLB) wishes to express thanks to the Deutsche Forschungsgemeinschaft for support

during his leave from Southern Illinois University. We also are grateful to Dr. V. Dose for making available his time-of-flight computer equipment.

APPENDIX: EXPERIMENTAL ERRORS

The possible error in the absolute cross sections measured is due to a variety of sources. Long-term variations in the photon count, which were caused by surface effects in the metastable source, at the windows of the gas filter cell, and the electron multiplier, could have caused an error in the absolute cross section of about ±15%. It should be noted, however, that these fluctuations did not affect the shape of the cross section because of the high repetition rate of the metastable beam pulse.

The possible uncertainty in the target-gas density was ±30%. This together with the above uncertainty results in a possible error in the absolute cross section of about ±50%. (The vertical error bars shown in Fig. 5 and Fig. 6 are due only to counting statistics and were insignificant compared with the total uncertainty in the absolute cross section.)

The horizontal error bars shown in Fig. 5 and Fig. 6 were caused by a variety of uncertainties in the kinetic energy of the O(^{5}S) metastables. These uncertainties are summarized briefly in the following (see Ref. 18 for further details.)

One uncertainty in the energy scale was caused by the thermal motion of the target-gas molecules. It was found by varying the optical viewing region and observing the resulting changes in signal intensity, that the velocity distribution of these molecules was Maxwellian and isotropic in three dimensions, as expected. Based on this fact, the relative velocities between beam particles and target-gas molecules were calculated. The standard deviation in the beam velocity v was found to be $\Delta v = \pm (kT/m_T)^{1/2}$, where k is the Boltzmann constant, T the absolute temperature of the target gas, and m_T the mass of the target molecules. The uncertainty Δv arises solely from the thermal motion of the target gas. Converting to the corresponding uncertainty in the kinetic energy of the beam particles, one obtains

$$\Delta E = \pm (2kTEm/m_T)^{1/2}, \tag{A1}$$

where E is the kinetic energy of the metastables and m their mass.

A second uncertainty in the kinetic energy arose from the finite temporal width of the metastable beam pulses. Using square pulses, the standard deviation for the uncertainty in time was found to be $\Delta t = \pm a/\sqrt{3}$ and the corresponding uncertainty in kinetic energy

$$\Delta E = \pm (a/3s)(2E)^{3/2}/\sqrt{3}, \tag{A2}$$

where t is the time of flight, a the half-width of the beam pulse, and s the distance between metastable source and target cell.

A third uncertainty in the kinetic energy was caused by the finite spatial width of the viewing region in the target cell (see also Fig. 1). Neglecting solid-angle effects and assuming a rectangular spatial distribution function for the viewing region, we found the standard deviation in the distance s to be $\Delta s = \pm b\sqrt{3}$ and the corresponding uncertainty in kinetic energy is

$$\Delta E = \pm (b/\sqrt{3}s)2E, \tag{A3}$$

where b is half the length of the viewing region. The calculations performed in arriving at Eqs. (A1)–(A3) are not valid for all data points. They hold generally for Eqs. (A1) and (A3) and below 4 eV for Eq. (A2). Above this energy, the result from Eq. (A2) may be inaccurate by about 10%.

The combined uncertainty from the three contributions above is shown by the horizontal error bars in Figs. 5 and 6. Typical individual uncertainties were 0.23 eV from Eq. (A1), 0.43 eV from Eq. (A2), and 0.10 eV from Eq. (A3) at a kinetic energy of 2 eV in the laboratory frame.

The finite time-of-flight channel width was neglected in the above determination of the uncertainty in the kinetic energy, since it was much smaller than the width of the beam pulse. The spatial dimensions of the metastable source were also neglected, since they were much smaller than the length of the optical viewing region in the target cell.

The broadening in the metastable kinetic energies has an effect on the rise in the cross sections shown in Figs. 5 and 6. This broadening was studied near the threshold in the cross section by assuming a step function for the cross section and convoluting it with the Maxwellian velocity distribution of the target gas and simultaneously the width of the beam pulse. The spatial extent of the viewing region was neglected in this calculation, since its error near threshold is smallest. The step function was positioned at a kinetic energy which gave the best fit of the convoluted curve to the low-energy tail of the experimental curve. The height of the step was normalized to the maximum in the experimental cross section. A rectangular velocity distribution for the metastables in the beam was assumed as a rough approximation (which is valid for TOF channel numbers greater than 6).

The calculations showed that the slope of the calculated cross section at the center of the rise

in Fig. 5 was larger by a factor of 1.5 than the measured slope. This means that the actual cross section rises more steeply than that measured in the present work. But it also shows that the actual cross section has a finite slope near threshold and cannot be represented by a step function with an infinite slope. The apparatus used would have been capable of measuring steeper slopes than those observed. However, it seems likely that the curvature in the cross section near threshold was due at least in part to the experimental broadening effects described.

---

*On leave from Southern Illinois Univ., Carbondale, Ill. 62901.

[1]C. D. Cooper, G. C. Cobb, and E. L. Tolnas, J. Mol. Spectrosc. 7, 223 (1961).
[2]D. L. Cunningham and K. C. Clark, J. Chem. Phys. 61, 1118 (1974).
[3]R. J. Donovan and D. Husain, Chem. Rev. 70, 489 (1970).
[4]D. L. Huestis, R. A. Gutschek, R. M. Hill, M. V. McCusker, and D. C. Lorents, Stanford Research Institute Technical Report No. 4 MP 15-18, 1975 (unpublished).
[5]H. T. Powell, J. R. Murray, and C. K. Rhodes, Appl. Phys. Lett. 25, 730 (1974).
[6]R. F. Heidner III, D. Husain, and J. R. Wiesenfeld, J. Chem. Soc. Faraday Trans. 2. 69, 927 (1972).
[7]R. F. Heidner III, D. Husain, and J. R. Wiesenfeld, Chem. Phys. Lett. 16, 530 (1973).
[8]H. D. Wolf, thesis, Physikalisches Institut der Universität Würzburg, 1976 (unpublished).
[9]H. D. Wolf and J. Fricke, Dtsch. Phys. Ges. 2, 122 (1976).
[10]W. L. Borst and E. C. Zipf, Phys. Rev. A 4, 153 (1971).
[11]R. S. Freund, J. Chem. Phys. 54, 3225 (1971).
[12]G. Nowak, W. L. Borst, and J. Fricke, in *Electronic and Atomic Collisions*, edited by M. Barat (Commissariat a l'Energie Atomique, Paris, 1977), Vol. I, p. 554.
[13]G. Nowak, thesis, Physikalisches Institut der Universität Würzburg, 1977 (unpublished).
[14]G. Nowak, W. L. Borst, and J. Fricke, Phys. Rev. A 17, 1921 (1978).
[15]W. L. Borst, G. Nowak, and J. Fricke, Phys. Rev. A 17, 838 (1978).
[16]J. Windrich, H. D. Wolf, and J. Fricke, J. Phys. B 11, 1235 (1978).
[17]J. Fricke, H. K. Kiefl, and W. L. Borst, Proceedings of the Thirty-First Annual Gaseous Electronics Conference, Buffalo, New York, 1978 (unpublished), p. 142.
[18]H. U. Kiefl, thesis, Physikalisches Institut der Universität Würzburg, 1978 (unpublished).
[19]H. U. Kiefl and J. Fricke, Verh. Dtsch. Phys. Ges. 2, 406 (1978).
[20]H. U. Kiefl and J. Fricke (unpublished).
[21]V. Dose and A. Richard (to be published).